Eletrônica de Potência
Open Journal of Power Electronics

Received July 03, 2024; accepted November 24, 2024; Date of publication December 15, 2024.
The review of this paper was arranged by Associate Editor Fabio Andrade and Editor-in-Chief Heverton A. Pereira.

Digital Object Identifier http://doi.org/10.18618/REP.e202456

Simple Method to Estimate Battery Lifetime and Upkeep of Lead-Acid and Lithium-Ion Batteries

Pedro C. Bolsi[1,2], **Edemar O. Prado**[1,2], **Romario J. Nazaré**[2], **Hamiltom C. Sartori**[1], **José R. Pinheiro**[1,2]

[1]Universidade Federal de Santa Maria, Santa Maria - RS, Brasil
[2]Universidade Federal da Bahia, Salvador - BA, Brasil

e-mail: pedrobolsi@ufba.br, edemar.prado@ufba.br, romario.jesus@ufba.br, hamiltomsar@gmail.com, jrenes@gepoc.ufsm.br

ABSTRACT This work provides an event-oriented method to model and predict the lifetime of lead-acid and lithium-iron phosphate batteries. An ampere-hour integration method is proposed to be used in conjunction with the event-oriented method to achieve higher accuracy. The methods are applied to lead acid and lithium-iron phosphate batteries on a commercial 1 kW single-office/home-office uninterruptible power supply (UPS). Additional circuits for measurements, or microprocessors are avoided to not increase the UPS cost, reducing its market competitiveness. The usefulness of the proposed approach is demonstrated by an upkeep analysis based on the cost of the battery and the service time for each battery technology.

KEYWORDS Lead-acid battery, Lifetime, Lithium ion, Lithium-iron phosphate, State of health, Uninterruptible Power Supply.

I. INTRODUCTION

Lead-acid batteries are the most common rechargeable battery type in the world [1], with some of its main applications being related to energy storage in emergency supply systems, photovoltaic applications and uninterruptible power supplies (UPS) [2]–[4]. On the other hand, lithium-ion batteries have been increasingly used in these systems, due to its superior characteristics of gravimetric and volumetric energy density [5].

Other battery technologies have been studied as alternatives to lead-acid and lithium-ion on battery storage systems: sodium-sulfur, nickel-cadmium, zinc-bromide and redox flow (vanadium). However, each of these has at least one disadvantage that prevents wide commercial use [6]. Sodium-sulfur batteries have typical operating temperatures above 300 °C, in order for sodium and sulfur to become liquid, thus not being viable for many applications. Nickel-cadmium batteries are prone to self discharge, suffer from memory effect, and its components are highly toxic for the environment when improperly discarded/not recycled. Zinc-bromide batteries have lower energy density, efficiency and slower charging and discharging speeds when compared to lithium-ion technology. Lastly, redox flow batteries have self discharge issues, caused by the low ion selectivity of its electrode separation membrane, leading to low efficiency and fast decay.

Consequently, lead-acid batteries are predominantly utilized in a wide range of power capacities in commercial UPS systems [7]–[13]. However, more recent UPS products are versatile, enabling them to employ lithium-ion or lead-acid batteries [14]–[16]. Among lithium-ion battery technologies, lithium-iron phosphate (LFP), despite its relatively lower energy density, is the go-to technology for UPS manufacturers, due to its improved safety and lifetime [17].

Although UPSs rely on battery-supplied operation exclusively during grid anomalies or failures, batteries remain susceptible to degradation even in standby mode, with lead-acid (LA) batteries being particularly affected. Generally, the degradation of all battery technologies is influenced by factors such as temperature, frequency and depth of discharge cycles, and the adopted charging process [18], [19].

The primary internal mechanisms responsible for the aging of LA batteries are electrode corrosion, active mass degradation, loss of adhesion of the active mass paste to the lead grid, internal short circuits, loss of water, and irreversible sulfation of the active mass [20]. In contrast, the main internal mechanisms that damage lithium ion batteries include lithium plating [21]–[24] and the growth of the solid-electrolyte interphase [22], [25], [26]. Lithium-ion batteries exhibit a less pronounced self-discharge phenomenon, with a rate of 1% per month at 30 °C [27], [28], compared to lead-acid batteries, which have a self-discharge rate of 5% per month [29], [30] at the same temperature. Consequently, certain LFP battery manufacturers list float charging as optional [31].

Due to the various internal mechanisms that contribute to battery degradation, the aging process is uniquely manifested in different applications. Consequently, for an accurate prediction of battery lifetime, it is essential to verify the state-of-health (SoH) to determine current battery conditions and prevent potential problems related to battery failure.

The state-of-health of a battery is defined as:

$$SoH = \frac{C_m}{C_r} \quad (1)$$

where C_m is the present maximum capacity of a battery (at full charge) and C_r the rated capacity of a new battery, specified by the manufacturer. The instantaneous capacity (C) can be used to determine the C_m of a battery through discharge:

$$C(t) = \int_0^{t_d} i_d(t)dt \quad (2)$$

where i_d is the discharge current and t_d is the discharge duration.

When the *SoH* of a battery reaches 80%, by definition, the lifetime has expired. In the literature, there are several approaches to lifetime modeling, which can be grouped into two categories: post-processing and performance degradation models [32].

Post-processing models predominantly utilize manufacturer-supplied data, making them the most accessible. These models encompass Ah-throughput counting [33] and event-oriented approaches [34], [35]. The Ah-throughput counting model is predicated on quantifying the charge passing through the battery, applying certain weights or stress factors. In contrast, the event-oriented model cumulatively accounts for the degradation in battery lifetime attributable to discrete events. Thus, the event-oriented methodology presupposes that each event affecting battery lifetime contributes linearly to its degradation. This approach assumes that incidents of abnormal or improper battery operation, which would significantly impair battery health, do not occur. Examples of such detrimental practices include discharges below the cut-off voltage, prolonged periods of low state-of-charge, or incomplete battery charging.

Performance degradation models are intended to represent battery degradation more accurately and comprehensively, using information on voltage, current, temperature, and capacity. Mainly, two methods are employed: equivalent circuit models or physico-chemical models [32]. The former approach uses circuit parameters (voltage sources, capacitances, resistances) to characterize the voltage behavior at the battery terminals [36]–[38], being continuously adjusted depending on the operating conditions of the battery [39]. Physico-chemical models, on the other hand, describe the internal state of the battery at a microscopic level, exhibiting higher complexity and necessitating a detailed understanding of the battery construction [34], [40], [41]. The intrinsic complexity of both equivalent circuit and physico-chemical models, compounded by the limited availability of manufacturer data, often impedes their application in lifetime modeling.

Considering these factors, this work proposes the employment of event-oriented and Ah-throughput counting post-processing techniques to predict battery lifetime and state-of-health, respectively, and integrates both methodologies.

Taking into account these factors, this work proposes the use of event-oriented and Ah-throughput counting post-processing techniques to predict battery lifetime and state-of-health, respectively, and integrates both methodologies. The methods are applied to an 1 kW uninterruptible power supply for single-office/home-office applications. These UPSs employ a single-phase inverter, typically powered by 12 V or 24 V battery banks, and are characterized by low power ratings (up to 1.5 kVA) [42], [43]. Since these UPS are competitive for their simplicity, small size, and cost-benefit, the use of new circuits, additional measurements, and advanced microprocessors is avoided [44].

To demonstrate the usefulness and relevance of the proposed method for practicing engineers, the estimated lifetime values are associated to the costs of lead-acid and lithium-iron phosphate batteries to perform an upkeep analysis. Examples are presented for different locations, correlating the operational conditions of the UPS product (including the temperature and the frequency of grid interruptions) with the optimal battery choice.

The manuscript is organized as follows. Section II provides a concise overview of the UPS system. Section III elucidates the procedure for SoH verification utilizing Ah-throughput. Section IV details the methods employed to estimate the lifetime of lead-acid and lithium-iron-phosphate batteries. Section V presents the results of the lifetime estimations for different locations in Brazil. Section VI concludes the manuscript.

II. SMALL-OFFICE/HOME-OFFICE (SOHO) UPS

The described application is a line-interactive UPS of 1 kW and an output voltage of 120 V RMS, designed for SOHO applications. In backup mode, it operates utilizing a battery voltage of 24 V and a single conversion stage. The voltage at the inverter output is increased by a low-frequency transformer [42], [45].

Figure 1 illustrates the operation and circuit of the UPS system. The low-frequency transformer provides galvanic isolation for the load from both the grid and the converter. In the event of significant surges or drops in grid voltage, the grid is disconnected and the load is powered by a pair of 12 V / 7 Ah VRLA batteries connected in series, through the full-bridge inverter. When the voltage of the grid remains within 120 ± 20 % V RMS, the load is powered by the grid through the transformer, while the full-bridge converter operates as a rectifier, charging the batteries and maintaining a floating charge.

The battery current measured during discharge ($i_d(t)$), for a 600 W load at the UPS output, is depicted in Figure 2. There is a significant current ripple at 120 Hz caused by the inverter operation. This $i_d(t)$ makes C_r levels of the UPS different than those provided by the manufacturer's data sheets, because they are obtained under different conditions.

Due to the natural behavior of battery discharge, the voltage at the battery terminals (v_{ter}) will decrease its

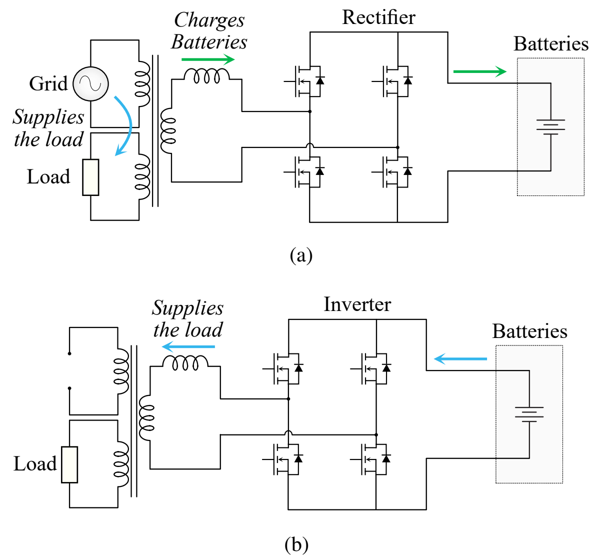

FIGURE 1. Case study ferroresonant SOHO UPS operation. (a) Grid-mode operation. (b) Backup-mode operation.

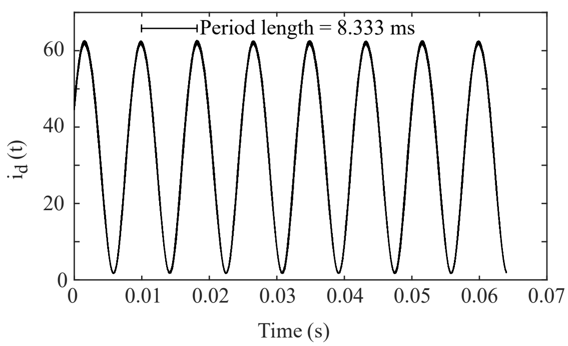

FIGURE 2. Waveform of i_d measured on the case study UPS, with a 600 W load at the output.

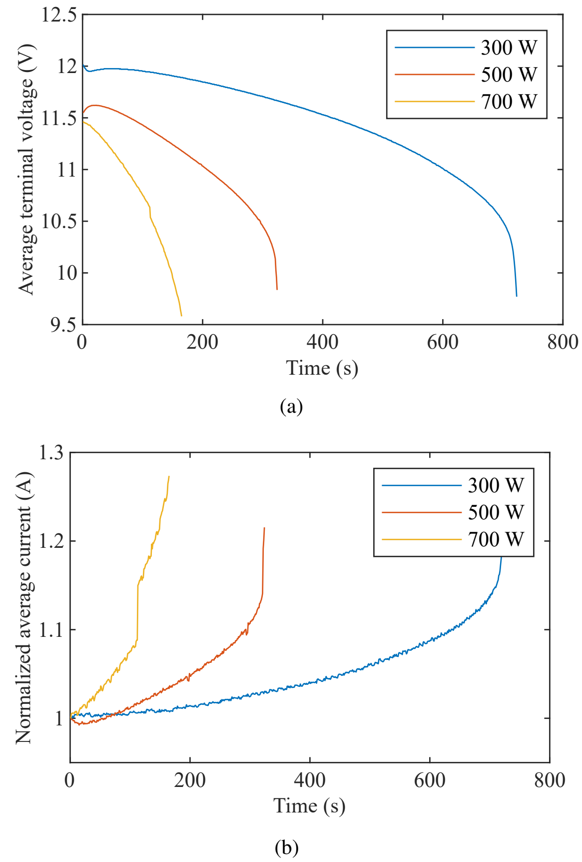

FIGURE 3. Average values measured on battery terminals during discharge. (a) Average voltage. (b) Average current (normalized).

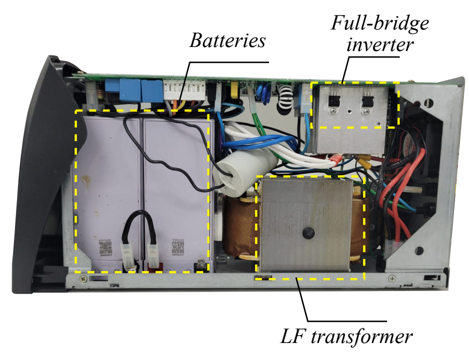

FIGURE 4. Case study UPS.

average value (V_{ter}) over time (Figure 3 (a)). Consequently, the average current (I_d) will increase over time (Figure 3 (b)). Figure 3 shows the behavior of V_{ter} and I_d for different loads on the UPS output. I_d is normalized by its initial value ($t = 0$), which corresponds to 14.8 A for 300 W, 25.8 A for 500 W and 36.9 A for 700 W.

Instantaneous waveforms are measured using a Tektronix DPO3034 oscilloscope. The Yokogawa WT1803E power analyzer is used to measure average and RMS voltages and currents. Temperature measurements are conducted with a Keysight DAQ970A datalogger equipped with type K thermocouples. Figure 4 presents the UPS case study with an open cabinet, illustrating its circuits.

III. STATE-OF-HEALTH VERIFICATION METHOD

Ampere-hour integration constitutes a fundamental method for analyzing the battery capacity. For real time *SoH* estimation under different load conditions, the value of C_r will vary according to different discharge currents [39]. Consequently, different C measurements obtained under varying i_d conditions require a set of C_r for an accurate application (1). By discharging a battery at different currents, a straightforward reference table can be developed. Table 1 details the values C_r obtained from the discharge of the case study battery (when with $SoH = 1$) connected to the UPS circuit.

The applicability of the reference values in Table 1 is illustrated by the discharge profiles depicted in Figure 5, where the case study battery is compared with an aged battery under identical load conditions at the UPS output. Using these reference values, the *SoH* of the aged battery is:

$$SoH = \frac{0.96}{3.1} = 0.309. \tag{3}$$

TABLE 1. Values of C_r obtained by discharge

UPS output load	$\overline{I_d}$ (A)	C_r (Ah)
200 W	10.36	3.7
300 W	15.49	3.1
400 W	20.81	2.8
500 W	26.86	2.4
600 W	33.43	2.0
700 W	40.29	1.8

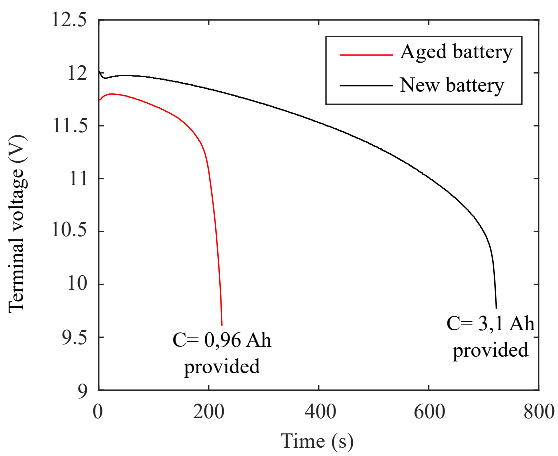

FIGURE 5. Discharge of two batteries with different *SoH* with a 300 W load at UPS output. Battery temperature is at 26 °C.

For comparison, a constant current test is conducted, and the measured C is compared to the value of C_r shown in the manufacturer's tables for constant current. The *SoH* obtained for the same battery was 0.319 with $I = 12$ A, indicating a discrepancy of 3.2%.

IV. LIFETIME ESTIMATION METHOD

The event-oriented methodology is used to model and predict battery lifetime. The temperature-sensitive degradation resulting from discharge cycles (D_{cyc}) and float time (D_{flt}) is integrated into an overall degradation metric D_T,

$$D_T = D_{cyc} + D_{flt} \tag{4}$$

where D_T, D_{cyc} and D_{flt} are percentages of lost *SoH*,

$$SoH = 1 - D_T. \tag{5}$$

A. Temperature adjustment

Temperature is a critical determinant of battery aging. With each 10 °C increase above the reference temperature, the degradation of the battery approximately doubles, leading to a roughly 50% decrease in the battery lifetime [46]. Manufacturers often present these data through graphs that correlate useful life (in years) with temperature [19], [47]. From these graphs, a temperature-stress factor τ can be derived:

$$\tau = q_1 e^{q_2 T} \tag{6}$$

where T is the battery temperature and q_1 and q_2 are coefficients obtained by curve fitting the manufacturer curve. This stress factor is applied to both D_{cyc} and D_{flt}.

B. Damage by cycles

The methodology used to estimate the *SoH* damage incurred by each battery cycle is based on the assumption that the tolerance of a battery to cyclical usage is a function of the depth of discharge (*DoD*). Manufacturers present these data in graphs that correlate different cycle counts with specified *DoD* values [19], [48]. Using these curves, the number of remaining cycles (R_{cyc}) according to the *DoD* can be modeled, and then translated into a specific amount of degradation per cycle (d_{cyc}) in percentage:

$$R_{cyc} = ae^{-a_1 DoD} + be^{-b1_D oD} \tag{7}$$

$$d_{cyc} = \frac{20}{R_{cyc}} \tag{8}$$

where a, b, a_1 and b_1 are obtained by curve fitting the manufacturer provided curve. A factor of 20 appears in the numerator because 20% is the amount of damage to *SoH* that indicates the end of the useful life.

The total battery damage caused by cycles over a period of time is then:

$$D_{cyc} = (\sum_{i=1}^{n} d_{cyc})\tau \tag{9}$$

where i is the number of cycles that occurred in the evaluated time interval, up to n. The effect of temperature on the damage caused by cycles is included by multiplying the degradation by τ.

C. Calendar aging

1) Lead-acid batteries

The calendar aging of LA batteries is modeled using the float degradation curves provided in the manufacturer catalogs. There is a relationship between the fluctuation time and the maximum battery charge retention capacity (or *SoH*). Through this relationship, it is possible to obtain an expression to estimate the remaining *SoH* of a lead-acid battery (SoH_R) as a function of the elapsed time (years):

$$SoH_R = A\ e^{-A_1 y \tau} + B\ e^{-B_1 y \tau} \tag{10}$$

where y is the time passed in years. A, B, A_1 and B_1 are curve fitting coefficients. The influence of temperature (τ) on the float life is included in the exponent A_1 and B_1. Then, the damage caused by float time is:

$$D_{cal,LA} = 1 - SoH_R. \tag{11}$$

2) Lithium-iron phosphate batteries

In the context of lithium-ion batteries, the remaining useful life is typically characterized as a function of the remaining number of cycles. Consequently, this characterization often neglects the degradation that occurs during periods of inactivity or standby (*standby*) [49], [50]. This phenomenon can be attributed partly to the low self-discharge rate of lithium-ion batteries, and partly to the nature of their predominant applications, such as electric vehicles, portable electronics, and power tools, which typically involve continuous battery cycling. Moreover, it is uncommon for lithium-ion battery manufacturers to disclose degradation during standby periods [27], [28], [51]–[54], in contrast to lead-acid manufacturers who routinely report useful life reductions during float charging [29], [55].

However, even without manufacturer-provided data, such information is critical for UPS applications, where batteries predominantly remain in standby mode, passing through few cycles. Therefore, in this work, the storage aging data presented in [50] are used to predict the calendar aging of LFP batteries, according to the expression,

$$D_{cal,LFP} = 3.087 \cdot 10^{-7} e^{0.05146(T+273)} t_m^{0.5} \tag{12}$$

where t_m is the operating time in months. Since this expression already considers the impact of temperature, the application of τ from (6) is not made.

Table 2 presents the coefficients for the application of equations (6), (8), and (10). These are obtained from the manufacturer curves.

TABLE 2. Coefficients for lifetime estimation, obtained from manufacturer data for LA [29] and LFP [27].

Coefficient	Value	Corresponding Equation
q_1	0.1768	(6)
q_2	0.06931	(6)
a (LA)	1225.9	(8)
a_1 (LA)	0.874	(8)
b (LA)	1528.8	(8)
b_1 (LA)	0.025	(8)
a (LFP)	9558	(8)
a_1 (LFP)	129.7	(8)
b (LFP)	0.003	(8)
b_1 (LFP)	0.0001	(8)
A (LA)	99.815	(10)
A_1 (LA)	1.380	(10)
B (LA)	-0.009	(10)
B_1 (LA)	-1.527	(10)

V. RESULTS

The proposed method for estimating the lifetime is demonstrated using five example cases. As an indicator of the continuity of energy supply, the Brazilian Electricity Regulatory Agency (ANEEL) provides data on the number of Equivalent Frequency of Interruptions by Consumer Unit (FEC) for each electricity supplier.

The moving average of the annual FEC by 2023 is used to estimate the number of battery discharges per year in different Brazilian states. These values are displayed in Table 3. The acronym of the electricity supply company from which the data is included. Since the employed method assumes that each event affects lifetime linearly, the average annual temperature of the capital of each state is used as the temperature reference. To emulate the inside of the UPS, an offset of 10°C is added to the ambient temperature, as measured in experiments. An average DoD of 80% is considered for the cycles.

TABLE 3. Moving average FEC values in different Brazilian cities and states.

City, State, Supplier	Annual FEC	Average Temperature
Salvador, Bahia, COELBA	13.14, round to 14	26.4°C
Manaus, Amazonas, AME	48.7, round to 49	27°C
Belo Horizonte, Minas Gerais, CEMIG	9.59, round to 10	21.5°C
São Paulo, São Paulo, CPFL	6.41, round to 7	20.4°C
Porto Alegre, Rio Grande do Sul, RGE	10.54, round to 11	19.9°C

The lifetime estimation is translated into an expected amount of battery replacements over a certain period. Based on this result, an upkeep analysis is performed considering the following costs for each pair of 12 V / 7 Ah batteries: 2×73.50 BRL (Brazilian Real) for LA, and 2×433.80 BRL for LFP. These values are used illustratively and are derived from quotations provided by a Brazilian manufacturer.

Figure 6 presents battery health damage for the city of Salvador considering (a) LA batteries, (b) LFP batteries. It is shown that, using the event-oriented method, cycle damage accumulates linearly, and calendar aging exponentially. The expected lifetime of an LA battery (from new) is 2.14 years, and of an LFP battery is 5 years. Taking these values as an estimate for the frequency of battery replacements, the annual upkeep may be calculated as,

$$\text{Upkeep} = \frac{\text{Battery pair cost}}{\text{Estimated lifetime}} \tag{13}$$

which for LA batteries is of 68.70 BRL per year, and for LFP batteries it is 173.50 BRL per year. This result shows that, based on the quoted costs, while LFP batteries are technologically superior, they still lose economically to LA for Salvador.

A similar analysis is conducted for Manaus, as illustrated in Figure 7. For this locality, the estimated operational lifetime is 1.5 years for LA and 4.25 years for LFP. Although the average temperature in Manaus is similar to that in Salvador, the number of battery cycles is significantly higher. Under these conditions, LFP batteries exhibit superior resilience as a result of their superior cycle performance. However, the annual maintenance cost for LA remains 98.00 BRL, which is lower than the 204.60 BRL required for LFP.

An analysis including all cities listed in Table 3 is presented in Figure 8. The annual upkeep costs for each battery technology are compared, along with the ratio among them. Although the cost of LFP batteries is 5.9 times higher than

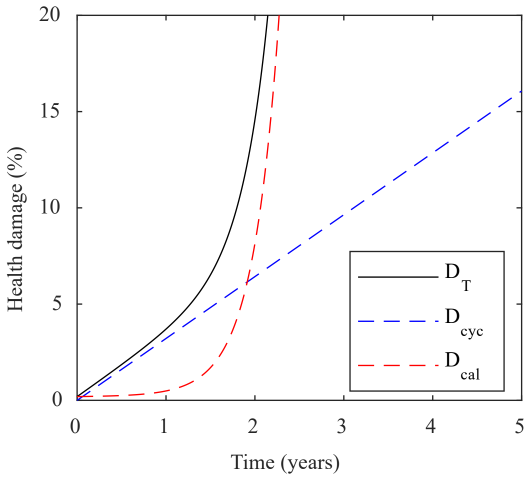

(a)

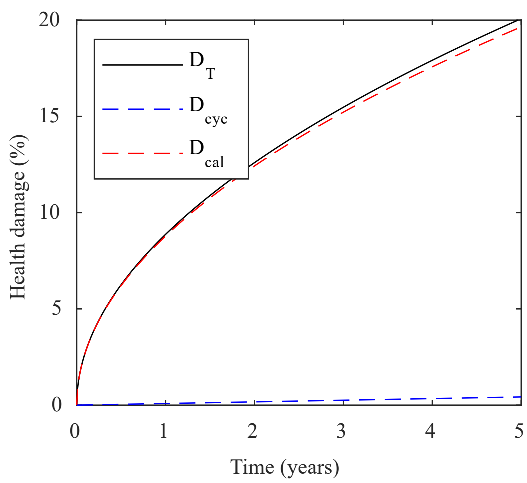

(b)

FIGURE 6. Lifetime prediction for the city of Salvador. (a) LA batteries. (b) LFP batteries.

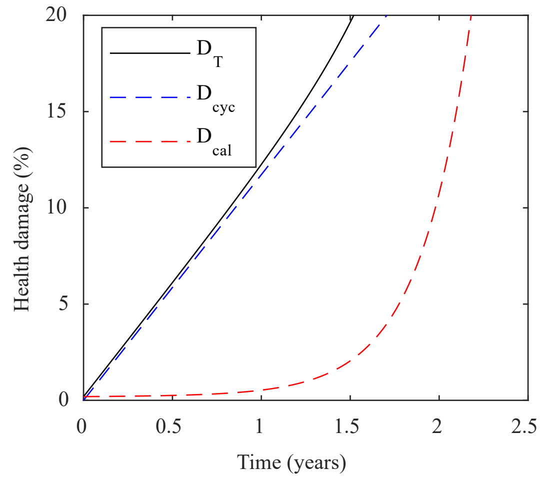

(a)

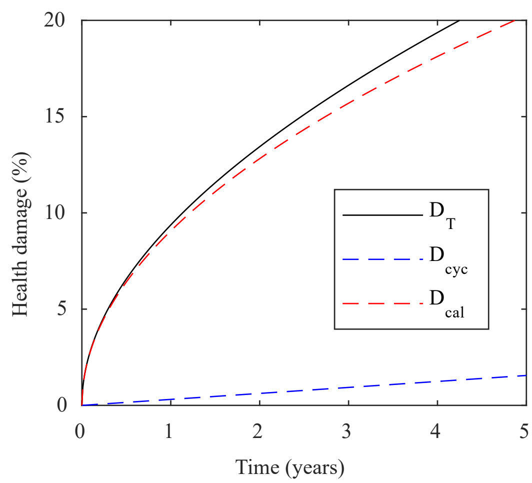

(b)

FIGURE 7. Lifetime prediction for the city of Manaus. (a) LA batteries. (b) LFP batteries.

LA, when considering the upkeep, the difference reduces to a value between 2 and 2.5, depending on the location.

The previous analysis was conducted assuming fresh (*SoH* = 100%) batteries. For a battery with an unknown *SoH*, its current degradation can be mapped to the calendar aging curve using the equation (5). The SoH required can be determined by measuring *SoH* through ampere-hour integration, as detailed in Section III. Subsequently, the current D_T is located in the curves derived from equations (8) through (12), based on the expected temperature and discharge profile.

For example, based on the degradation predictions illustrated in Figure 6, the remaining lifetime can be easily determined through a *SOH* measurement. Assuming a *SoH* identification rate of 90% for both batteries, the projected remaining lifetime is approximately 4 months for LA batteries and approximately 3 years and 9 months for LFP batteries. The comparative analysis of the results underscores the technological superiority of LFP batteries in terms of lifetime.

VI. CONCLUSION

In this work, an event-oriented method for predicting battery lifetime was presented. Its accuracy is supported by the verification of the state-of-health of the battery, which is feasible after each discharge with constant load. In addition, the post-processing attributes of the event-oriented method have been improved. Furthermore, the methods are compatible with the SOHO UPS application, which demonstrates particular discharge characteristics.

The proposed methods offer significant utility for professional designers and engineers due to their simplicity and exclusive dependence on manufacturer-provided data, thereby eliminating the need for comprehensive laboratory testing and characterization of batteries. In addition, its cost

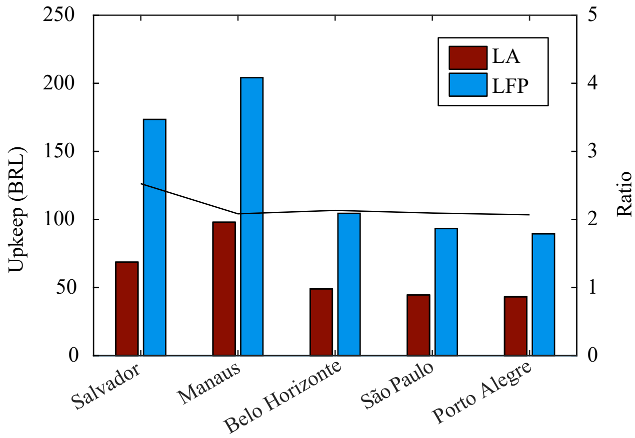

FIGURE 8. Battery technology annual upkeep comparison, for each city.

effectiveness, stemming from the absence of requirements for advanced microprocessors, supplementary circuits, or additional measurements, enhances the market competitiveness of the case study UPS product.

An analysis of upkeep costs was conducted to compare the two prevailing battery technologies utilized in UPS products, lead-acid and lithium-iron phosphate. The findings indicate that although the latter exhibits superior performance, current pricing allows lead-acid batteries to maintain an economic advantage in terms of replacement costs. For batteries with equivalent voltage and ampere-hour ratings, the cost disparity between the two technologies is a factor of 5.9. However, when considering annual upkeep expenses, this disparity decreases to a range of 2 to 2.5, depending on the location. This difference is expected to decrease further as the market for lithium-iron phosphate batteries in UPS applications continues to grow.

ACKNOWLEDGMENT

This work was financially supported in part by the funding agencies CNPq and CAPES/PROEX Financing code 001.

AUTHOR'S CONTRIBUTIONS

P. C. BOLSI: Conceptualization, Data Curation, Formal Analysis, Funding Acquisition, Investigation, Methodology, Software, Validation, Visualization, Writing – Original Draft, Writing – Review & Editing. **E. O. PRADO:** Data Curation, Investigation, Writing – Original Draft, Writing – Review & Editing. **R. J. NAZARÉ:** Conceptualization, Formal Analysis, Investigation, Methodology, Software, Writing – Review & Editing. **H. C. SARTORI:** Formal Analysis, Funding Acquisition, Supervision, Validation, Writing – Review & Editing. **J. R. PINHEIRO:** Funding Acquisition, Project Administration, Resources, Supervision, Writing – Review & Editing.

PLAGIARISM POLICY

This article was submitted to the similarity system provided by Crossref and powered by iThenticate – Similarity Check.

REFERENCES

[1] M. Mann, V. Putsche, B. Shrager, *Grid Energy Storage-Supply Chain Deep Dive Assessment*, USDOE Office of Policy, 2022, doi:10.2172/1871557.

[2] S. Sabihuddin, A. E. Kiprakis, M. Mueller, "A numerical and graphical review of energy storage technologies", *Energies*, vol. 8, no. 1, pp. 172–216, 2014, doi:10.3390/en8010172.

[3] P. Nikolaidis, A. Poullikkas, "Cost metrics of electrical energy storage technologies in potential power system operations", *Sustainable Energy Technologies and Assessments*, vol. 25, pp. 43–59, 2018, doi:10.1016/j.seta.2017.12.001.

[4] E. O. Prado, P. C. Bolsi, H. C. Sartori, J. R. Pinheiro, "An Overview about Si, Superjunction, SiC and GaN Power MOSFET Technologies in Power Electronics Applications", *Energies*, vol. 15, no. 14, p. 5244, 2022, doi:10.3390/en15145244.

[5] A.-I. Stan, M. Swierczynski, D.-I. Stroe, R. Teodorescu, S. J. Andreasen, K. Moth, "A comparative study of lithium ion to lead acid batteries for use in UPS applications", *in 2014 IEEE 36th international telecommunications energy conference (INTELEC)*, pp. 1–8, IEEE, 2014, doi:10.1109/INTLEC.2014.6972152.

[6] M. Ratshitanga, A. Ayeleso, S. Krishnamurthy, G. Rose, A. A. Aminou Moussavou, M. Adonis, "Battery Storage Use in the Value Chain of Power Systems", *Energies*, vol. 17, no. 4, 2024, doi:10.3390/en17040921.

[7] Eaton Corporation, *9155 UPS*, 2013.

[8] WEG Electric Corp., *Nobreak Enterprise*, 2022.

[9] Legrand Group, *Keor SP UPS for offices and IT applications*, 2021.

[10] Schneider Electric, *SRT10KRMXLT - APC Smart-UPS SRT 10000VA RM 208V*, 2021.

[11] Legrand Group, *Keor HP Three-phase UPS*, 2014.

[12] Phoenix Contact GmbH, *QUINT4 - UPS/1AC/1AC/1KVA*, 2021.

[13] Schneider Electric, *SMT750I - APC Smart-UPS 750VA LCD 230V*, 2017.

[14] Voltronic, *Compact 1U 1KVA*, Voltronic Power Technology Corp, 2022.

[15] Schneider, *SRTL3KRM1UNC - APC Smart-UPS 3kVA Lithium-Ion*, Schneider Electric, 2023.

[16] Vertiv, *Liebert ITA2 UPS*, Vertiv Group Corp., 2023.

[17] W. Burgess, *Lithium batteries for UPS applications*, Eaton, January 2018.

[18] K. W. Beard, *Linden's Handbook of batteries*, vol. 5, McGraw-Hill, 2019.

[19] Panasonic, *VRLA Handbook*, 2021.

[20] P. Ruetschi, "Aging mechanisms and service life of lead–acid batteries", *Journal of Power Sources*, vol. 127, no. 1, pp. 33–44, 2004, doi:https://doi.org/10.1016/j.jpowsour.2003.09.052, eighth Ulmer Electrochemische Tage.

[21] T. Waldmann, J. B. Quinn, K. Richter, M. Kasper, A. Tost, A. Klein, M. Wohlfahrt-Mehrens, "Electrochemical, post-mortem, and ARC analysis of Li-ion cell safety in second-life applications", *Journal of The Electrochemical Society*, vol. 164, no. 13, p. A3154, 2017, doi:10.1149/2.0961713jes.

[22] P. Keil, S. F. Schuster, J. Wilhelm, J. Travi, A. Hauser, R. C. Karl, A. Jossen, "Calendar aging of lithium-ion batteries", *Journal of The Electrochemical Society*, vol. 163, no. 9, p. A1872, 2016, doi:10.1149/2.0411609jes.

[23] A. Tomaszewska, Z. Chu, X. Feng, S. O'kane, X. Liu, J. Chen, C. Ji, E. Endler, R. Li, L. Liu, *et al.*, "Lithium-ion battery fast charging: A review", *ETransportation*, vol. 1, p. 100011, 2019, doi:10.1016/j.etran.2019.100011.

[24] A. Ulvestad, "A brief review of current lithium ion battery technology and potential solid state battery technologies", *arXiv preprint arXiv:180304317*, 2018, doi:10.48550/arXiv.1803.04317.

[25] N. Takenaka, A. Bouibes, Y. Yamada, M. Nagaoka, A. Yamada, "Frontiers in theoretical analysis of solid electrolyte interphase formation mechanism", *Advanced Materials*, vol. 33, no. 37, p. 2100574, 2021, doi:10.1002/adma.202100574.

[26] T. Joshi, K. Eom, G. Yushin, T. F. Fuller, "Effects of dissolved transition metals on the electrochemical performance and SEI growth in lithium-ion batteries", *Journal of the electrochemical society*, vol. 161, no. 12, p. A1915, 2014, doi:10.1149/2.0861412jes.

[27] PowerTech Systems SAS, *PowerBrick+ 12 V Lithium-Ion Battery Pack*, 2022.

[28] SOLISE, *Batterie 24V 7,2Ah LiFePO4*, 2022.

[29] Acumuladores Moura SA, *Manual de Instalação e Operação Baterias Estacionárias VRLA*, 2021.

[30] WEG SA, *Manual do Usuário Baterias VRLA*, 2020.

[31] Vision Battery Inc., *Important Tips of Using Iron-V LiFePO4 Battery*, 2022.

[32] H. Bindner, T. Cronin, P. Lundsager, J. Manwell, U. Abdulwahid, I. Baring-Gould, *Lifetime modelling of lead acid batteries*, no. 1515(EN) in Denmark. Forskningscenter Risoe. Risoe-R, Forskningscenter Risoe, 2005.

[33] J. Schiffer, D. U. Sauer, H. Bindner, T. Cronin, P. Lundsager, R. Kaiser, "Model prediction for ranking lead-acid batteries according to expected lifetime in renewable energy systems and autonomous power-supply systems", *Journal of Power sources*, vol. 168, no. 1, pp. 66–78, 2007, doi:10.1016/j.jpowsour.2006.11.092.

[34] D. U. Sauer, H. Wenzl, "Comparison of different approaches for lifetime prediction of electrochemical systems—Using lead-acid batteries as example", *Journal of Power sources*, vol. 176, no. 2, pp. 534–546, 2008, doi:10.1016/j.jpowsour.2007.08.057.

[35] R. Dufo-López, J. M. Lujano-Rojas, J. L. Bernal-Agustín, "Comparison of different lead–acid battery lifetime prediction models for use in simulation of stand-alone photovoltaic systems", *Applied Energy*, vol. 115, pp. 242–253, 2014, doi:10.1016/j.apenergy.2013.11.021.

[36] I. A. Azzollini, V. Di Felice, F. Fraboni, L. Cavallucci, M. Breschi, A. Dalla Rosa, G. Zini, "Lead-acid battery modeling over full state of charge and discharge range", *IEEE Transactions on Power Systems*, vol. 33, no. 6, pp. 6422–6429, 2018, doi:10.1109/TPWRS.2018.2850049.

[37] C. Burgos, D. Sáez, M. E. Orchard, R. Cárdenas, "Fuzzy modelling for the state-of-charge estimation of lead-acid batteries", *Journal of Power Sources*, vol. 274, pp. 355–366, 2015, doi:10.1016/j.jpowsour.2014.10.036.

[38] F. Sun, R. Xiong, H. He, "A systematic state-of-charge estimation framework for multi-cell battery pack in electric vehicles using bias correction technique", *Applied Energy*, vol. 162, pp. 1399–1409, 2016, doi:10.1016/j.apenergy.2014.12.021.

[39] P. C. Bolsi, E. O. Prado, A. C. C. Lima, H. C. Sartori, J. R. Pinheiro, "Battery autonomy estimation method applied to lead–acid batteries in uninterruptible power supplies", *Journal of Energy Storage*, vol. 58, p. 106421, 2023, doi:10.1016/j.est.2022.106421.

[40] R. Xiong, J. Cao, Q. Yu, H. He, F. Sun, "Critical review on the battery state of charge estimation methods for electric vehicles", *Ieee Access*, vol. 6, pp. 1832–1843, 2017, doi:10.1109/ACCESS.2017.2780258.

[41] S. K. Rahimian, S. Rayman, R. E. White, "State of charge and loss of active material estimation of a lithium ion cell under low earth orbit condition using Kalman filtering approaches", *Journal of the Electrochemical Society*, vol. 159, no. 6, p. A860, 2012, doi:10.1149/2.098206jes.

[42] E. O. Prado, P. C. Bolsi, H. C. Sartori, J. R. Pinheiro, "Comparative Analysis of Modulation Techniques on the Losses and Thermal Limits of Uninterruptible Power Supply Systems", *Micromachines*, vol. 13, no. 10, p. 1708, 2022, doi:10.3390/mi13101708.

[43] E. O. Prado, P. C. Bolsi, H. C. Sartori, J. R. Pinheiro, "Design of Uninterruptible Power Supply Inverters for Different Modulation Techniques Using Pareto Front for Cost and Efficiency Optimization", *Energies*, vol. 16, no. 3, p. 1314, 2023, doi:10.3390/en16031314.

[44] P. C. Bolsi, E. O. Prado, R. J. Nazaré, H. C. Sartori, J. R. Pinheiro, "Simple Method to Estimate Battery Lifetime of Lead-Acid and Lithium-Ion Batteries in Uninterruptible Power Supplies", *in 2023 IEEE 8th Southern Power Electronics Conference and 17th Brazilian Power Electronics Conference (SPEC/COBEP)*, pp. 1–6, 2023, doi:10.1109/SPEC56436.2023.10408219.

[45] M. K. Rahmat, A. Z. A. Karim, M. N. M. Salleh, "Sensitivity analysis of the AC uninterruptible power supply (UPS) reliability", *in 2017 International Conference on Engineering Technology and Technopreneurship (ICE2T)*, pp. 1–6, IEEE, 2017, doi:10.1109/ICE2T.2017.8215976.

[46] T. M. Layadi, G. Champenois, M. Mostefai, D. Abbes, "Lifetime estimation tool of lead–acid batteries for hybrid power sources design", *Simulation Modelling Practice and Theory*, vol. 54, pp. 36–48, 2015, doi:10.1016/j.simpat.2015.03.001.

[47] Power-Sonic Co., *PG-12V9*, 2018.

[48] Amara Raja Batteries, *HUPS 12V - 160 AH*, 2019.

[49] H. Tian, P. Qin, K. Li, Z. Zhao, "A review of the state of health for lithium-ion batteries: Research status and suggestions", *Journal of Cleaner Production*, vol. 261, p. 120813, 2020, doi:10.1016/j.jclepro.2020.120813.

[50] D.-I. Stroe, M. Świerczyński, A.-I. Stan, R. Teodorescu, S. J. Andreasen, "Accelerated Lifetime Testing Methodology for Lifetime Estimation of Lithium-Ion Batteries Used in Augmented Wind Power Plants", *IEEE Transactions on Industry Applications*, vol. 50, no. 6, pp. 4006–4017, 2014, doi:10.1109/TIA.2014.2321028.

[51] Vision Battery Inc., *Iron-V LFP12-10EV (12V 10Ah)*, 2020.

[52] ELB, *Lithium Ion Phosphate Battery 12.8 V 10 Ah*, 2022.

[53] Green Cell, *GC LiFePO4 Battery CAV09 7 Ah 12.8 V*, 2022.

[54] Bioenno Power, *BLF-1208LB LiFePO4 Battery 12 V 8 Ah*, 2019.

[55] Unicoba, *Manual técnico bateria estacionária*, 2021.

BIOGRAPHIES

Pedro Cerutti Bolsi holds master's (2020) and PhD (2024) degrees in Electrical Engineering from the Federal University of Santa Maria (UFSM), and pursues a PhD in Electrical Engineering at the Federal University of Bahia (UFBA). Currently employed as a Senior Research Engineer at Collins Aerospace in Cork, Ireland. His research interests include design and optimization of power converters, modeling of magnetic components, power electronics filter design, batteries, and EMI filter design.

Edemar de Oliveira Prado holds master's (2020) and PhD (2024) degrees in Electrical Engineering from the Federal University of Santa Maria (UFSM). Currently, he is pursuing a Ph.D. in Electrical Engineering at the Federal University of Bahia (UFBA). From 2023 to 2024, he completed a sandwich Ph.D. in France, collaborating with the Gustave Eiffel University and the VEDECOM Institute. He has experience in the area of Electrical Engineering, working mainly on the following topics: Renewable energy sources integrated into UPSs and ESSs; Evaluation of modulation techniques, thermal design, and converter optimization; Design, modeling, and control of dynamic wireless power transfer systems for electric vehicles.

Romario de Jesus Nazaré completed his master's degree in Electrical Engineering at the Federal University of Bahia (UFBA) in 2024. Currently, he is pursuing a Ph.D. in Electrical Engineering at UFBA. He has experience in the area of Electrical Engineering, working mainly on the following topics: Power electronics; interleaved boost converter, mathematical modeling of converters, interleaved converter control, sliding mode control.

Hamiltom Confortin Sartori holds master (2009), doctorate (2013) and post-doctorate (2016) degrees in Electrical Engineering at the Federal University of Santa Maria – Brazil. Currently is adjunct professor of the electrical energy processing department at the Federal University of Santa Maria – Brazil. Has experience in power electronics, acting mainly in optimized design of power converters, high voltage gain converters, uninterruptable power supplies, magnetic component design, semiconductors (selection, loss analysis and heat transfer system design), renewable energy sources, batteries and electromagnetic compatibility (EMI).

José Renes Pinheiro holds a degree in Electrical Engineering from the Federal University of Santa Maria/UFSM (1981), a master's degree in Electrical Engineering from the Federal University of Santa Catarina/UFSC (1984), a doctorate in Electrical Engineering from UFSC (1994), and a post-doctorate from Virginia Tech, VA, USA (2002). Since 2018, he has been a visiting professor at the Federal University of Bahia in the Department of Electrical Engineering. He has experience in the area of Electrical Engineering, with an emphasis on Power and Control Electronics, working mainly on the following topics: Hybrid Multilevel Converters, UPS, modeling and control of static converters, systems integration and soft switching techniques, power supplies, and distributed electrical energy generation systems. He is a member of SOBRAEP and IEEE (PELS, IAS, IES and PES).